bioresources.com

Experimental Study of the Behavior of Box Floor with Orthogonal Ribbed Beams by Poplar LVL

Hongwei Ma,[a] Anlian Wang,[a] Jialong Ji,[a] Yan Liu,[a,*] and Meng Gong [b]

Considering the unidirectional layout of ribbed beams and simple structure in traditional wooden floors, it is not suitable for large-span wooden buildings. Six groups of floor ribbed beams with plane size of 4.8 m×3.6 m were designed and manufactured by using poplar laminated veneer lumber (LVL), among which five floor specimens were orthogonal ribbed beams and the other one was traditional. A bending performance test was carried out to analyze the influence of different ribbed beam spacing and high span ratio on the mechanical performance of poplar LVL orthogonal ribbed beams, and its results were compared with that of the traditional floor with ribbed beams. The results showed that the box floors with orthogonal ribbed beams had good integrity during the bending process. Moreover, the change of the high span ratio had an important influence on the bending performance of the box floors with orthogonal ribbed beams, and the change of the spacing of the ribbed beams had a relatively small influence on the flexural performance of the box floors with orthogonal ribbed beams. Under the same conditions, the bending performance of the box floors with orthogonal ribbed beams was better than that of traditional floor.

*Contact information: a: College of Architectural Science and Engineering, Yangzhou University, Yangzhou, Jiangsu 225127 P. R. China; b: Wood Science and Technology Center, University of New Brunswick, Fredericton, New Brunswick E3C 2G6 Canada; *Corresponding authors: liuyan@yzu.edu.cn*

INTRODUCTION

Poplar laminated veneer lumber (LVL) is an engineering wood material, which is made of small diameter logs by rotary cutting, drying, gluing, forming blanks parallel to the grain direction, and gluing. This type of lumber is characterized by high yield, stable lumber quality, and high mechanical property (Gilbert *et al.* 2019).

There have been many studies on the physical and mechanical properties of poplar LVL. Liu and Yang (1997) tested the physical and mechanical properties of poplar LVL and found uniform material properties and little variation. Colakoglu (2004) analyzed the physical and mechanical properties of poplar LVL made of different materials and colloids and found that different types of glue resulted in different strength characteristics. Hirofumi *et al.* (2010) conducted tests on poplar LVL made of five kinds of wood, and the strength of poplar LVL was related to the direction of wood texture. Cui *et al.* (2016) carried out physical performance tests and reported that the bending performance of fiber line implantation was significantly improved. Meng *et al.* (2016) conducted tests on strength of poplar LVL made of poplar and eucalyptus with different veneer thickness and found that

the strength of poplar LVL increased with the decrease of veneer thickness.

Many research studies have focused on the topic of the wooden floor cover. Chen *et al*. (2004) examined the reinforcement detected results of actual wooden floor cases and concluded that the design of the wooden floor should consider the strength, deformation, feasibility, and the convenience for construction. Paquette and Bruneau (2006) conducted quasi-dynamic tests on full-size wooden floors and found that there was no obvious plastic deformation on the wooden floors. Pathak and Charney (2008) simulated floor under lateral loads and found that nail connection was the main source of in-plane flexibility, independent of the aspect ratio of floor. Zhou *et al*. (2008) conducted a vibration performance test on an 8.26×6.09 m wooden floor with truss joists and found that the vibration performance of the wooden floor could be significantly improved by adding transverse bracing and slatted bracing. Li *et al*. (2010) established a finite element model of wooden floor and reported that a simplified wooden floor model can be used to analyze the hybrid structure and design. Sadashiva *et al*. (2011) investigated the influence of the deflection changes of the wooden floor in the plane on its structural response and found that the single-layer structure was most affected by its deflection. Chen (2015) conducted tests on three composite wooden floors of 3.66 m × 4.88 m and found that transverse bracing and the arrangement of reinforced thin steel belt could improve the shear performance of these composite wooden floors. Further research on poplar LVL floor is necessary due to the relatively few studies on this topic.

Based on the research of traditional floor with ribbed beams, the floors with poplar LVL orthogonal ribbed beams were tested on the structure of orthogonal bidirectional bending properties and compared to the deflection results of wooden floors with orthogonal ribbed beams by the method of bidirectional board (GB50010-2010; Liu *et al*. 1997), quasi plate method, and cross beam line method (Shen 2003; Bai 2018). The research results provide reference for the experimental research and theoretical analysis of poplar LVL box floor and expands the application of poplar LVL material in building structure.

EXPERIMENTAL

Test Specimens

To investigate the influence of depth-span ratio and ribbed beam spacing on the behavior of the orthogonal ribbed beams of the wooden-floor, six floors specimens, which were designated as L1 to L6 in Table 1, were designed according to Chinese codes (GB50005-2012; GB50005-2017) and fabricated with the following variables: (1) with orthogonal ribbed beams (L1, L2, L3, L4, and L5) or without orthogonal ribbed beams (L6); (2) the plane dimensions of all six floors were 3600 mm×4800 mm; (3) different depth-span ratio of ribbed beams; (4) different ribbed beam spacing of wooden floors; and (5) the width of four side beams of all six floors were 80 mm, and the length of these side beams was the same as that of ribbed beams of every floor. The depth-span ratio of specimens L1, L2, L3, L4, and L5 were equal to 0.392, 0.261, 0.196, 0.308, and 0.475, respectively. The height of ribbed beams of specimens L1, L2, L3, and L6 was 235 mm, but that of specimens L4 and L5 were 185 mm and 285 mm, respectively (Fig. 1a). Specimen L6 had transversal beams with spacing of 600 mm and longitudinal diagonal braces (30×50 mm) with spacing of 1200 mm (Fig. 1b), which served as a control specimen. The effect of depth-span ratio on the ribbed beam behavior can be obtained by comparing the performance of Specimens L1, L2, L3, L4 and L5. The effect of ribbed

beam spacing on the ribbed beam behavior can be seen by comparing L1, L2, and L3. The transverse ribbed beam axis was numbered from left to right, the longitudinal ribbed beam axis was numbered from bottom to top with English letters, and the axis numbers of test pieces L1 and L6 are shown in Fig. 4 and Fig. 5.

All ribbed beams of six specimens (the longitudinal beams are full length, and the transverse beams are truncated by longitudinal beams) were fabricated using poplar LVL produced by Jiangsu Jiuhe Wood Industry Company. The coupon tests were conducted at Yangzhou University to determine the physical and mechanical properties of the materials (Liu *et al.* 2017; Su *et al.* 2022) (Table 2). There were three types of steel connectors (3-mm thickness) between ribbed beams; they were manufactured using steel Q235B (Ma *et al.* 2019; Ma *et al.* 2020) with yield stress of 235 MPa, which included internal node connector, end node connector, and angle connector (Liu *et al.* 2022). Self-tapping screws (M4×20) were used to connect the beams and connectors (Fig. 1), whose spacing and relative position between them are shown in Fig. 2.

Table 1. Specimen Design Parameters

Number	Plain Dimension (m)	Ribbed Beam Spacing (mm)	Rib Beam Section Size (mm)	Depth-Span Ratio	Ribbed Beam Layout
L1	3.6×4.8	600	40×235	0.392	Bidirectional
L2	3.6×4.8	900	40×235	0.261	Bidirectional
L3	3.6×4.8	1200	40×235	0.196	Bidirectional
L4	3.6×4.8	600	40×185	0.308	Bidirectional
L5	3.6×4.8	600	40×285	0.475	Bidirectional
L6	3.6×4.8	600	40×235	0.392	Unidirectional

Table 2. Physical and Mechanical Properties of Poplar LVL

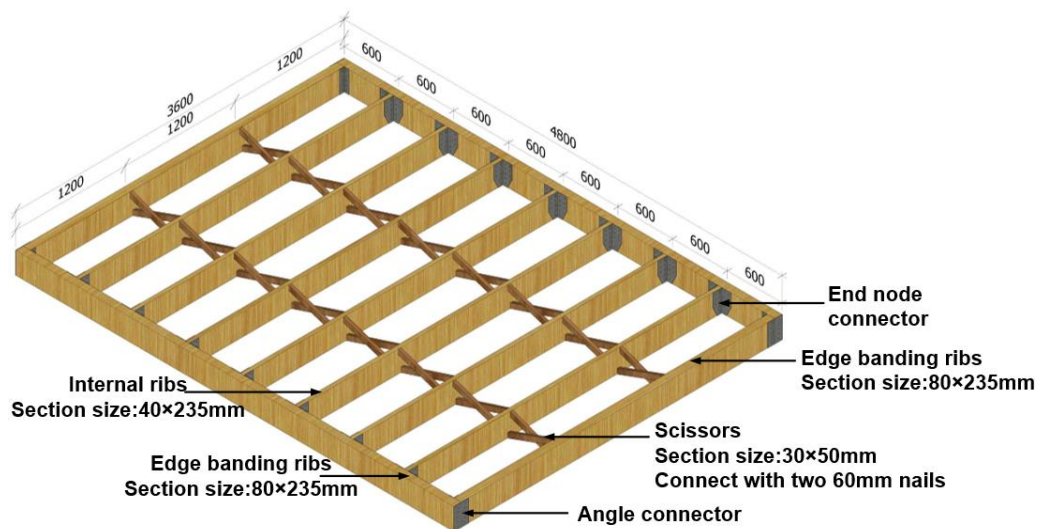| Moisture Content (%)	12.8
Density (g/cm^3)	0.576
Tensile Strength along Grain (MPa)	39.4
Compressive Strength along Grain (MPa)	37.03
Horizontal Grain Compressive Strength (MPa)	6.3
Bending Strength of Glue Layer (MPa)	Level 61.56
	Vertical 64.8
Flexural Modulus of Elasticity (MPa)	Level 9877.3
	Vertical 10135.4

Test Setup

The ribbed beams, L-shaped steel connectors with and self-tapping screws used for the flexural test are shown in Figs. 1 and 3. In selecting the beams, connectors, and screws, the elastic method was used in designing ribbed beams. The physical and mechanical properties of poplar LVL, whose material performance tests were carried out in the material

laboratory of Yangzhou University, are given in Table 2. The six specimens were fabricated by a local fabricator and all tests were performed in accordance with the Chinese specification (GB/T 50329-2012). In the actual test, the loading device of this test adopts a self-designed steel frame support and water tank system. The water tank is composed of a steel frame, whose height is 1200 mm, and plastic canvas with 1300 mm internal height. The purpose of the 100-mm difference between water tank height and internal height is to fit on the ribbed beams of the floor, so that the load acts evenly on the floor ribbed beam and deforms together with the ribbed beams. The bottom of the water tank fits the ribbed beam of the specimen to ensure uniform stress. The support adopts a steel support frame that can be assembled and disassembled. The whole test device was shown in Fig. 3.
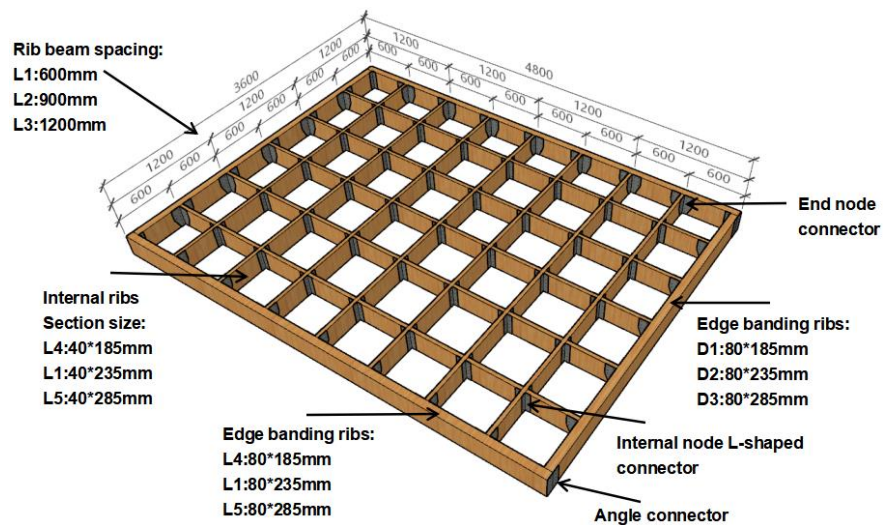
(a) Schematic diagram of ribbed beam layout of L1-L5 specimens

(b) Schematic diagram of ribbed beam layout of L6 specimen

(c) L1 specimen

(d) L6 specimen

Fig. 1. Schematic diagram of Poplar LVL orthogonal ribbed beam specimen

(a) Internal node connector

(b) End node connector

(c) angle connector

Fig. 2. Schematic diagram of node connectors of the specimens

Fig. 3. Water tank loading device

Test Apparatus

To measure the strain and deflection values of all levels of the specimens under the vertical uniformly distributed load, the test apparatus, whose arrangement would consider the symmetry of each specimen, consists of: (1) water tank to apply vertical load to the ribbed beams; (2) the flow meter control the applied load value by controlling water amount in the water tank; (3) a strong steel frame to support the floor and water tank; and (4) a strong floor to support the entire test assembly. As shown in Fig. 4, the instrumentation consists of: (1) The strain gauges at the bottom of the ribbed beam joints and bottom middle of longitudinal ribbed beams of quarter specimen to monitor the stress change; (2) the strain gauges at the middle bottom of transverse ribbed beam to analyze the stress working state of the short beams; (3) the linear variable displacement transducers (LVDT) (Wang *et al.* 2019) at the bottom of the longitudinal and transverse beam junctions in order to observe the change of joint deformation; (4) four dial indicators B1, B2, B3, and B4 at the middle of the four edge beams to measure the displacement change of the surrounding support ribbed beam. All loads, displacements, and strains were recorded in a data acquisition system at a rate of 60 channels per second. All recorded data were stored in a computer for subsequent analyses.

Loading Protocol

The tests were carried out according to the structures GB/T 50329 (2012) and ASTM E2322-03 (2015) standards. During pre-loading, the sample was loaded to 5% of the ultimate load (the ultimate load was calculated according to the finite element simulation results and calculation results), and the load holding was 15 min. During this period, the equipment and instruments were checked to see whether they were working normally, and then the water in the tank was evacuated for unloading. Before hierarchical loading, all measuring equipment should be zero. The loading value of the first stage was 10% of the ultimate load. From the second stage, loading value of each stage was increased by 5% of the ultimate load, and the loading holding time of each stage was 15 min. After the instrument reading was stable during the test, the test data and test phenomenon were record.

The test was stopped when the load of floor was less than 7.6 kN/m². This is based on the standard value of uniformly distributed live load on civil building floor, which is 2.0 kN/m² by Chinese specification (GB50009-2012), and the reliability of the test setup.
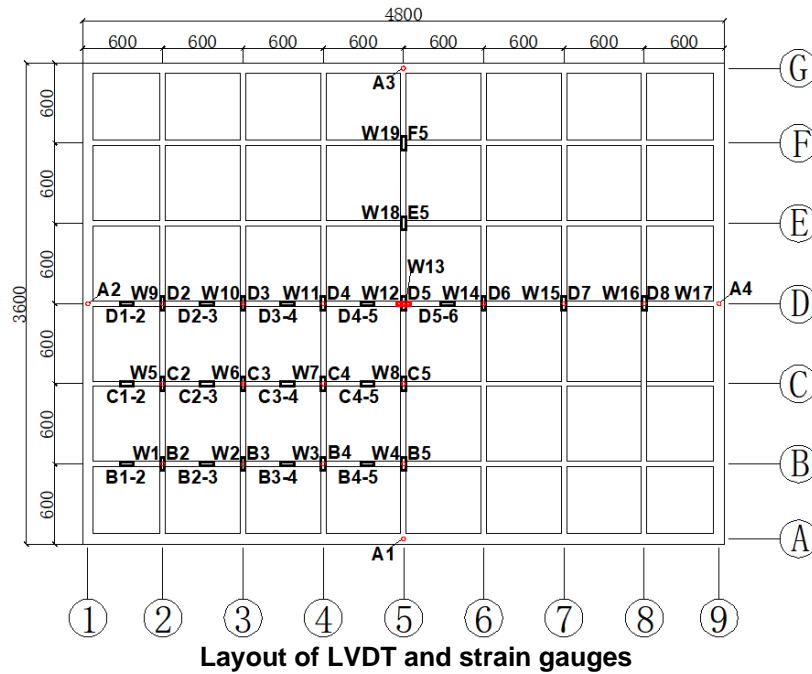
Fig. 4. Arrangement of measuring points of specimen L1
Note: "。" stands LVDT, represented by "W* and A*"; "▭" stands strain gauge, represented by "B*, B*-*,C*,C*- *,D*,D*- * and E*, F*".
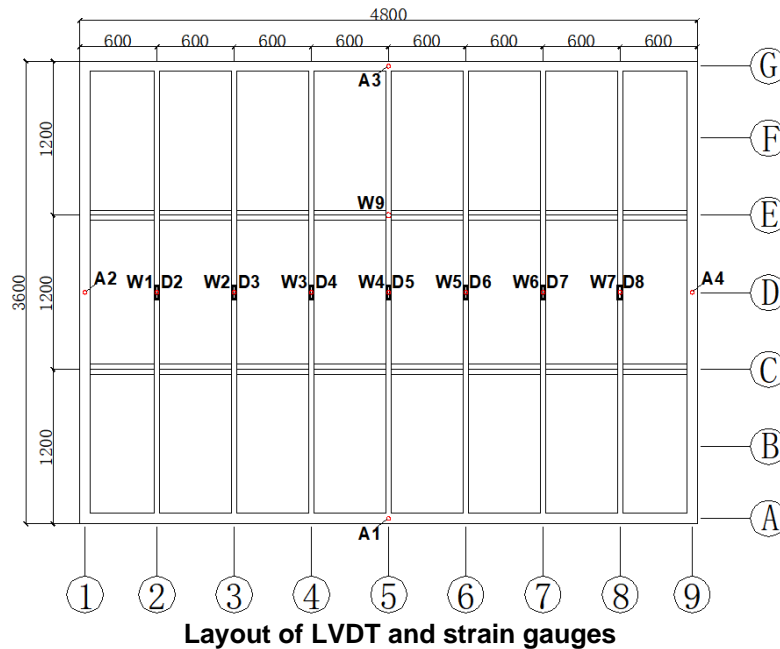
Fig. 5. Arrangement of measuring points of specimen L6
Note: "。" stands LVDT, represented by "W* and A*"; "▭" stands strain gauge, represented by "D*".

bioresources.com

General Behavior and Failure Pattern

The overall failure mode of all specimens was that the self-tapping screws in the metal connections connecting the cross ribbed beams were pulled out, resulting in partial separation of the cross ribbed beams at some joints. Some final failure modes are shown in Fig. 6.
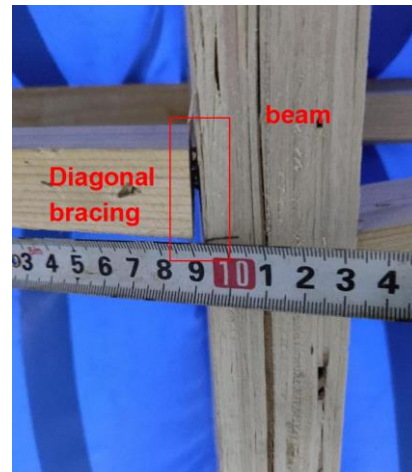

(a) The end of the ribbed beam is broken

(b) Cracking of internal ribbed beam joint

(c) Pull out the ribbed beam node screws

(d) The scissor brace is separated from the ribbed beam

Fig. 6. Test failure phenomenon of each specimen

The failure modes of each specimen are as follows:

(1) For specimen L1 with height span ratio of 0.392, when the load reached 7 kN/m^2, there was a slight crack in the edge beam at the joint of axis A and axis 5. When the load reached 7.5 kN/m^2, the self-tapping screws at the first node of axis D and axis 3 and at the second node of axis D and axis 7 were slightly pulled out and the dimension of the gaps between ribbed beams were 5 and 4 mm, respectively.

(2) For specimen L2 with height span ratio of 0.261, when the load reached 7.5 kN/m^2, the self-tapping screw at the first joint of axis C and axis 5 and the second joint of axis C and axis 3 and the third joint of axis C and axis 7 was lightly pulled out and the width of the gaps between ribbed beams were 9, 5, and 4 mm, respectively.

(3) For specimen L3 with height span ratio of 0.196, when the load reached 7.5 kN/m^2, the self-tapping screw at the first joint of axis B and axis 3 and the second joint of axis C and axis 7 was fractionally pulled out with a width of 5 mm.

bioresources.com

(4) For specimen L4 with height span ratio of 0.308, when the load reached 7.5 kN/m^2, three edge beams at the intersection of axis A and axis 4, and axis A and axis 5, and axis A and axis 6, were slightly torn, with a width of 2, 5.5, and 3.5 mm. The self-tapping screws at the intersection of axis D and axis 3, and axis D and axis 7 were slightly pulled out, and the ribbed beams were separated by 4 mm and 2.5 mm, separately.

(5) For specimen L5 with height span ratio of 0.475, when the load was loaded to 7.5 kN/m^2, there was no obvious structural damage, and the structural deflection was smaller than that of other specimens.

(6) For specimen L6 with height span ratio of 0.392, when the load reached 7.5 kN/m^2, the gap between the diagonal bracing and ribbed beam, which is between axis 2 and axis 3, was 4 mm.

The results indicate that the increase of height span ratio led to an increase in the bearing capacity of ribbed beams, and the reduction of ribbed beam spacing could effectively distribute the load of specimens. When the loading reached 7.5 kN/m^2, the self-tapping screws were pulled out from some of the joints of the specimen, and the connector separated from the ribbed beam, indicating the combination of joint failure mode and shear failure mode.

RESULTS AND DISCUSSION

Load-Strain Curve and Analysis

The load strain curve of poplar LVL orthogonal ribbed beam specimen in each box floor is presented in Fig. 7. The abscissa in the figures is the strain of the ribbed beam and the ordinate is the test loading value. From these figures, two observations can be drawn. First, for all specimens there was a linear relationship between load and strain at the initial stage, which was positive, indicating that the bottom of the ribbed beam was in flexural tension state.

In the whole deformation process of the orthogonal ribbed beam specimen, the longitudinal short-ribbed beams were conducive in reducing the deformation and the spatial torsion degree of transverse long-ribbed beams, and in improving the overall stiffness of the specimen. Second, all strain values of transversal ribbed beams were negative, illustrating that these ribbed beams bottom were under pressure.

For specimens L1, L2, and L3 with different ribbed beam spacing, when the applied load reached 45 to 60 kN, their curves became nonlinear for these three specimens with different parameters. In particular, the slope of curves increased by a gradual increase of ribbed beam spacing, but the strain growth rate increased. Meanwhile, the curves mutation increased and changed greatly with the increase of ribbed beam spacing because of a reduction number of self-tapping screws, and the weakening of connector constraints between ribbed beams, and sliding of some self-tapping screws. These results suggest that a densification of ribbed beams could lead to the rapid transmission and uniform distribution of load, and thus enhance a higher load.

In comparison with the traditional specimen L6, the maximum strain of the ribbed beam of the specimen L1 was reduced by 41.7% due to the existence of orthogonal ribbed beams. This result could greatly reduce section failure.
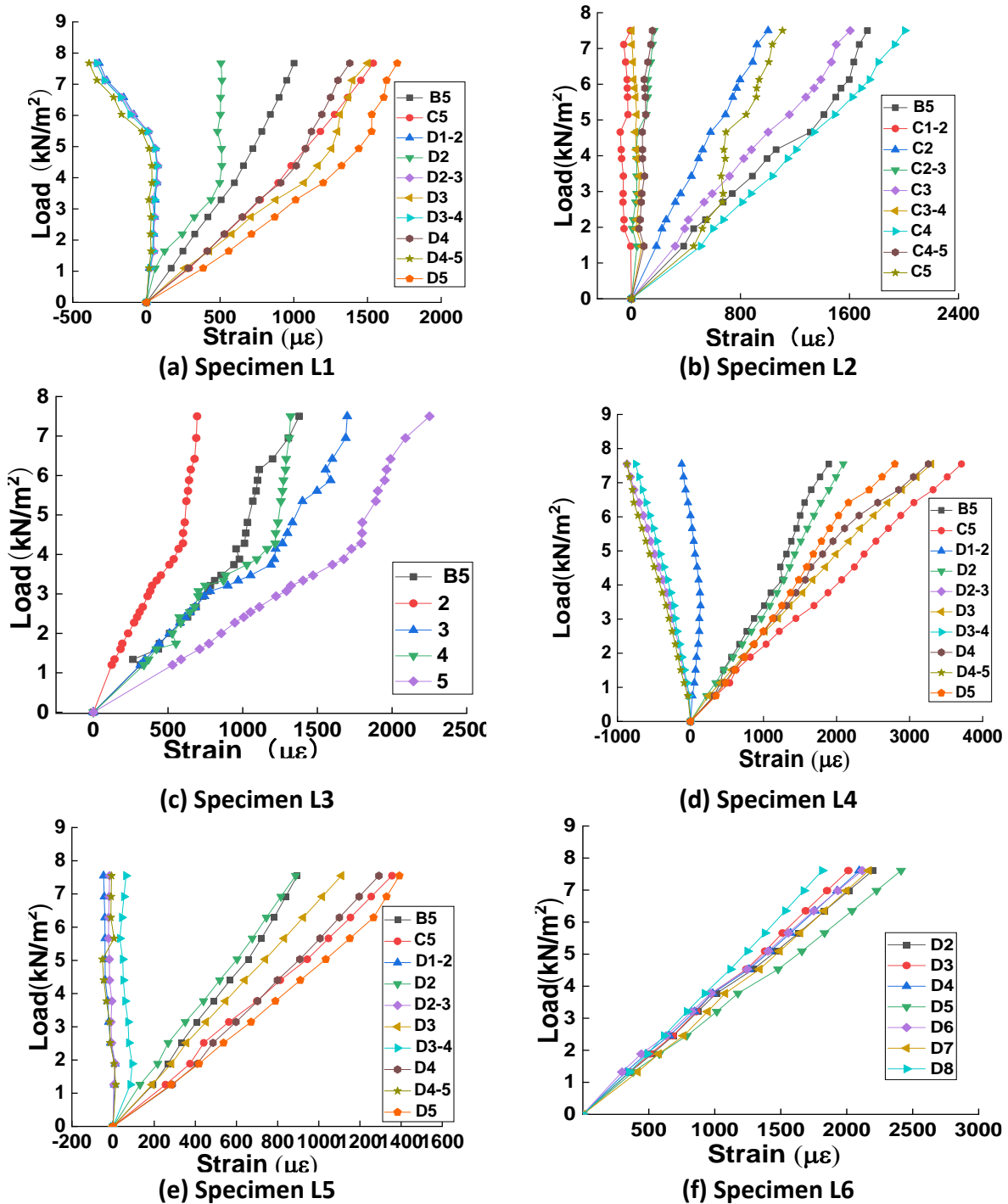
Fig. 7. Load-strain curve of each specimen

Deformation Analysis

Load-displacement analysis

According to the test results of six specimens, the relationship between load and displacement of each measuring point basically increased linearly, and the displacement value of measuring points at symmetrical positions was basically equal with small error. Among the test results, the maximum displacements of specimens L1, L2, L3, L4, and L5 were 25, 26, 28, 55, 18, and 31 mm, respectively. It can be seen from the results of specimens L1, L2, L3, and L6 that the change of height span ratio had a slight effect on the

bioresources.com

deflection of specimens. From the test results of specimens L1, L4, and L5, it can be seen that the change of beam height had a great impact on the deflection of the specimen because the number of self-tapping screws was reduced, resulting in the increase of shear force borne by a single self-tapping screw and sliding. Therefore, the number of self-tapping screws has become one of the factors controlling the deflection of the specimen. According to the vertical displacement data of each measuring point under the load of 7.5 kN/m^2, the deflection and deformation diagram of each floor ribbed beam is drawn, as shown in Fig. 8. The deflection deformation of poplar LVL orthogonal ribbed beam specimen is the largest in the middle of the span and decreases around the midpoint. The vertical deformation of the whole floor ribbed beam specimen is "bowl".
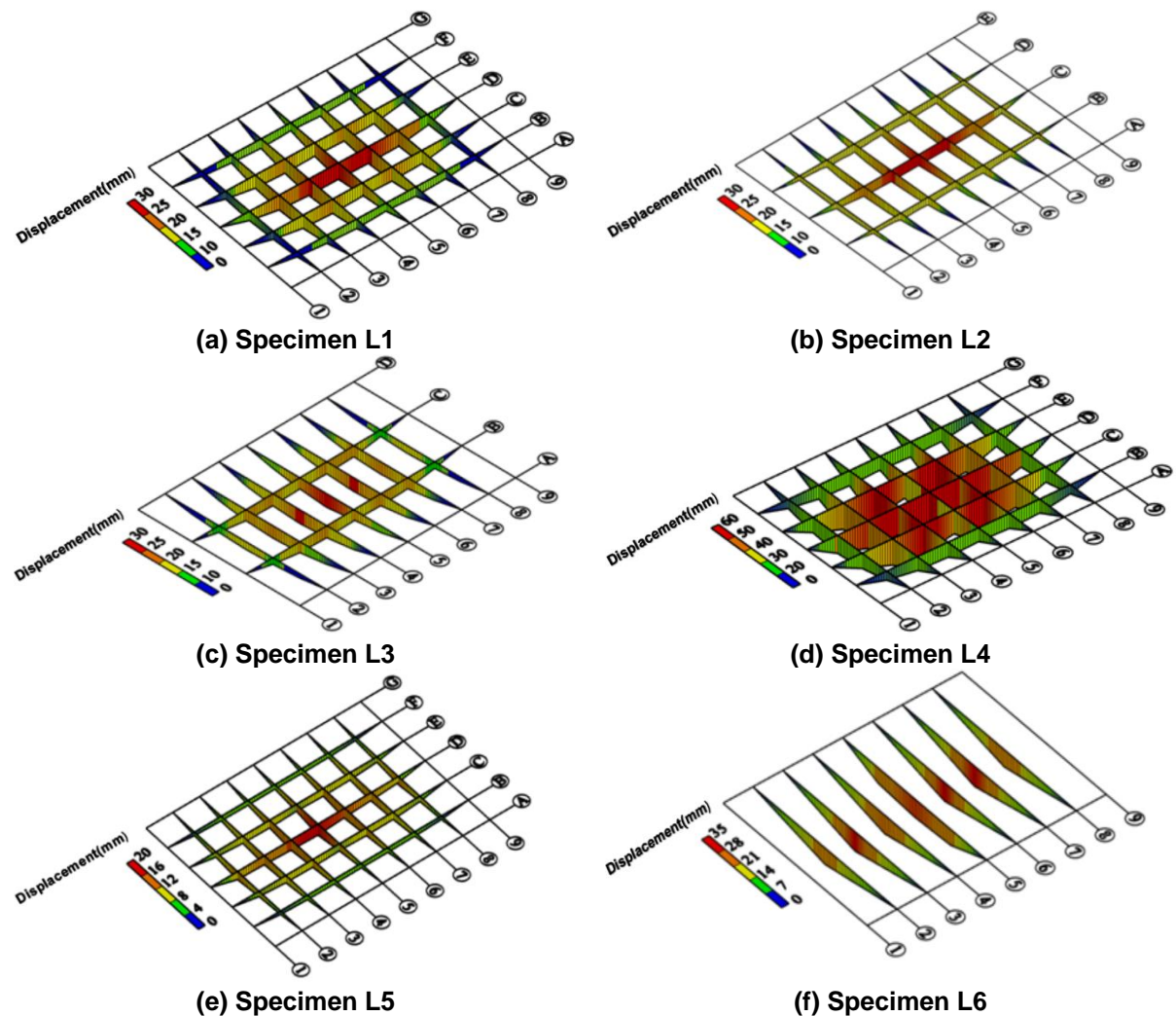

(a) Specimen L1

(b) Specimen L2

(c) Specimen L3

(d) Specimen L4

(e) Specimen L5

(f) Specimen L6

Fig. 8. Schematic diagram of deflection and deformation of each specimen

Deflection analysis

The maximum deflection of each specimen is shown in Table 3. The comparison of deflection values of all specimens shows that under normal service load (live load is 2.5 kN/m^2) (GB50009-2012), all specimens except D1 met the allowable deflection value requirements of flexural member ribbed beams specified in the literature (Ma *et al*. 2020). Under the same load (7.5 kN/m^2) (GB50009-2012), the deflection of L1 was 51.0% lower

than that of L4, and that of L5 was 33.2% lower than that of L1 when only the height of the ribbed beam was changed. For specimens L1, L4, and L5, the flexural rigidity of specimens increased by about 70% with each 50-mm increase in the sectional height of the ribbed beam. For specimens L1, L2, and L3, the change in the spacing of ribbed beams increased the stiffness of L1 by 11.3% compared with L3. In addition, the experiment also shows that the deflection of orthogonal floor ribbed beams (L1) was 19.5% lower, and the stiffness was 13.1% higher than that of traditional floor ribbed beams (L6) under the same condition of ribbed beam section height and load.

The maximum load in the table is the maximum load value added by the test, 7.5 kN/m^2; Normal service load is defined as the following: take the normal service limit load standard value combined with "constant load + live load" to calculate the floor uniformly distributed load (live load is 2.5 kN/m^2) (GB50009-2012). The allowable deflection value of floor beam of flexural members is set as L /250 as required.

Table 3. The Maximum Deflection of Each Specimen

Specimen Number	Maximum Load Deflection (mm)	Deflection Under Normal Load (mm)	Allowable Deflection (mm)	Relative Stiffness (N/mm)
L1	26.30	9.52	14.40	4538
L2	27.51	9.80	14.40	4408
L3	29.09	10.59	14.40	4079
L4	53.63	16.61	14.40	2601
L5	17.57	5.59	14.40	7728
L6	31.43	10.96	14.40	3942

Table 4. Numerical Table of Deflection of Ribbed Beam (unit:mm)

Section \ Position \ Deflection Value		0	0.6(0.9)	1.2	1.8	2.4	3(2.7)	3.6	4.2	4.8
Horizontal	L1	0.65	-5.00	-8.39	-9.47	-9.52	-9.46	-8.91	-5.80	0.72
	L2	0.68	-5.03	-7.34	-9.21	-9.80	-8.44	-8.33	-5.81	0.75
	L3	0.71	-6.10	-9.74	*	-10.59	-10.51	-9.77	-4.74	0.79
	L4	0.87	-10.91	-15.62	-16.60	-16.39	-15.64	-14.88	-8.86	0.89
	L5	0.43	-4.09	-4.81	-5.33	-5.59	-5.00	-3.91	-2.96	0.39
Vertical	L1	0.56	-4.56	-7.64	-9.52	-7.10	-5.01	0.53	-	-
	L2	0.58	-6.28	-	-9.80	-	-5.22	0.56	-	-
	L3	0.61	-	-9.42	-10.59	-7.48	-	0.61	-	-
	L4	0.72	-7.72	-13.61	-16.39	-12.69	-6.86	0.78	-	-
	L5	0.33	-2.48	-3.92	-5.59	-3.90	-2.10	0.36	-	-
Note:* The measuring point fails										

Analysis of stiffness of orthogonal ribbed beams

Because the A-G axis of the orthogonal ribbed beams is composed of short-ribbed beams, the longitudinal and transverse stiffness of the orthogonal ribbed beams is different. According to the deflection of longitudinal and transverse ribbed beams under general floor live load (2.5 kN/m^2), the difference value of longitudinal and transverse stiffness of the specimens of orthogonal ribbed beams (including the longitudinal direction along 3600 mm and the transverse direction along 4800 mm) was analyzed. The deflection value of each orthogonal ribbed beams is shown in Table 4.

Based on the basic principles of elasticity, when both constrained ends of the beam are the same, the deflection curve of a beam made of elastic material under uniform distributed load is a quartic parabola curve.

Quartic equation of horizontal ribbed beams:

L1: $y=0.21x^4-2x^3+7.6x^2-14x+0.75$

L2: $y=0.19x^4-1.8x^3+6.9x^2-13x+0.71$

L3: $y=0.29x^4-2.6x^3+9x^2-15x+0.39$

L4: $y=0.43x^4-4.2x^3+16x^2-28x+0.83$

L5: $y=0.14x^4-1.4x^3+5.6x^2-9.5x+0.31$

Quartic equation of vertical ribbed beams:

L1: $y=-0.047x^4+0.32x^3+2.2x^2-10x+0.58$

L2: $y=0.22x^4-1.8x^3+8x^2-16x+0.58$

L3: $y=-0.86x^4+5.7x^3-7.5x^2-6x+0.61$

L4: $y=-0.53x^4+3.6x^3-2.2x^2-14x+0.71$

L5: $y=-0.21x^4+1.5x^3-1.5x^2-3.8x+0.29$

According to the bending moment of the floor ribbed beam and the curvature of the fourth-order deformation curve, the relative stiffness of the longitudinal and transverse ribbed beam under uniformly distributed load can be obtained, the relative values of the stiffness of each specimen are calculated, and the results are shown in Table 5.

Table 5. Relative Values of Longitudinal and Longitudinal Stiffness of Orthogonal Ribbed Beam Specimens

Specimen Number	Relative Stiffness	
	Horizontal	Vertical
L1	1.50	1.70
L2	1.57	1.67
L3	1.50	1.51
L4	0.9	0.98
L5	2.80	3.02

As determined from the relative value of the stiffness of longitudinal and transverse ribbed beams in Table 5, the relative value of the stiffness of longitudinal ribbed beams in the specimens of all orthogonal ribbed beams was greater than the relative value of transverse ribbed beams. This was because the transverse ribbed beams were made of spliced short beams and the orthogonal ribbed beams were a whole beam without truncation. With the increase of the depth-span ratio of the ribbed beams, the relative value difference of longitudinal and transverse stiffness was about 9.6%. When the spacing of the ribbed beams varies, the relative value of the longitudinal and transverse stiffness of the specimens had a small difference. This was because the reduction of the number of transverse ribbed beams reduced the hindrance of the longitudinal ribbed beams in the other direction during the deformation process, resulting in relatively coordinated deformation of the joints among the ribbed beams.

Comparison of theoretical calculation and experimental values of deflection

Based on the cross beam system method (GB50010-2010; Liu *et al*. 1997), the Two-way plate method and the plate fitting method, the deflection deformation of the orthogonal ribbed beam structure system in the box floor of the poplar LVL was calculated theoretically by using the cross beam system method and the continuous plate system calculation method (two-way plate method and pseudo-plate method) (Shen 2003; Bai 2018), and the calculated results were compared with the test results. The results are shown in Table 6, where the mean relative error is the error between the theoretical value and the experimental value of each sample.

Compared with the test results, the average relative error of the calculation results based on the bidirectional board method was 7.2%, while the average relative error of the cross beam system and the simulated plate method were 26.8% and 26.5%, respectively. This was because the bidirectional board method took into account the load distribution in two directions and the deflection coordination at the midpoint of the slab. The cross beam system method considered the deflection coordination at all nodes, and the simulated plate method considered the deflection coordination of the whole ribbed beam. The deflection calculation of the orthogonal ribbed beam system of poplar LVL without covering the plate obtained by the bidirectional plate method was in good agreement with the experimental values.

Table 6. Comparison of Theoretical Calculation Deflection Value and Test Deflection Value (unit:mm)

Method \ Number	Load Value (2.5 kN/m²)					Load Value (7.5 kN/m²)					Average Relative Error (%)
	L1	L2	L3	L4	L5	L1	L2	L3	L4	L5	
Test value	9.52	9.80	10.59	16.61	5.59	26.30	27.51	29.09	53.63	17.57	-
Cross beam method	6.87	7.05	7.20	14.07	3.85	20.61	21.14	21.61	42.20	11.54	26.8
Bilateral plate method	9.48	9.48	9.48	19.41	5.31	28.41	28.45	28.45	58.14	15.91	7.2
Simulation	5.30	8.98	10.77	10.82	2.98	20.19	26.94	32.32	41.33	11.32	26.5

CONCLUSIONS

1. The box floor with orthogonal ribbed beams showed good integrity during the loading process, although the self-tapping screws were detached and cracks occurred between ribbed beams. The deflection deformation of the mid-span was the largest and decreased along the midpoint to the four sides. The vertical deformation of the whole floor was "bowl-shaped".

2. The change in the ratio of the height to span of the ribbed beams had a greater impact on the specimens of the orthogonal ribbed beams than the change in the spacing of the ribbed beams. For every 50-mm increase in the section height, the flexural rigidity of the specimens increased by about 70%.

3. The orthogonal ribbed beams benefited the stiffness of the specimens. Compared with the value of L6 specimens, the deflection of L1 specimens was reduced by 19.5%, and the stiffness increased by 13.1%, and maximum strain decreased by 41.7%.

4. The experimental deflection calculation of box floor with orthogonal ribbed beams made by poplar laminated veneer lumber (LVL) without covering panel was in good agreement with the values calculated by the bidirectional plate method.

ACKNOWLEDGMENTS

REFERENCES CITED

ASTM E2322-03 (2015). "Standard test method for conducting transverse and concentrated load tests on panels used in floor and roof construction," ASTM International, West Conshohocken, PA.

Bai, Z. (2018). *Research and Application of Multi-layer Large-Span Space Steel Grid Box Structure*, Guizhou University, Gui Yang, China.

Chen, T., Meng, Y., Zhang, W., and Gu X. (2004). "Case analysis of inspection and strengthening for a timber structural floor system," *Sichuan Building Science* 30(3), 39-41.

Chen, Z. (2015). *Investigation of the In Plane Shear Behavior of Diaphragms with Small-Diameter Timber Composite Joists*, Harbin Institute of Technology, Harbin, China.

Colakoglu, G. (2004). "A comparative study on some physical and mechanical properties of laminated veneer lumber (LVL) produced from beech (*Fagus orientalis* Lipsky) and eucalyptus (*Eucalyptus camaldulensis* Dehn.) veneers," *Holz Roh Werkst*, 62, 218-220. DOI: 10.1007/s00107-004-0464-3

Cui, J., Huang, H., Han, S., He, Y., and Jiang, G. (2016). "Influence of glass fiber implantation on the mechanical properties of poplar laminated veneer lumber," *Journal of Forestry Engineering* 1(5), 40-44. DOI: 10.13360/j.issn.2096-1359.2016.05.008

GB 50010-2010 (2010). "Code for design of concrete structures," Standards Press of China, Beijing, China.

GB 50005-2012 (2012). "Technical code of glued laminated timber structures," China Architecture & Building Press, Beijing, China.

GB 50005-2017 (2017). "Standard for design of timber structures," China Architecture & Building Press, Beijing, China.

GB/T 50329-2012 (2012). "Standard for test methods of timber structures," Standards Press of China, Beijing, China.

GB 50009-2012 (2012). "Load code for the design of building Structures," China Architecture & Building Press, Beijing, China.

Gilbert, B. P., Zhang, H., and Bailleres, H. (2019). "Reliability of laminated veneer lumber (LVL) beams manufactured from early to mid-rotation subtropical hardwood plantation logs," *Structural Safety* 78, 88-99. DOI: 10.1016/j.strusafe.2019.02.001

Hirofumi, I., Hirofumi, N., Kato, H., Miyatake, A., and Hiramatsu, Y. (2010). "Strength properties of laminated veneer lumber in compression perpendicular to its grain," *J. Wood Sci.* 56, 422-428. DOI: 10.1007/s10086-010-1116-3

Li, S., He, M., Guo S., and Ni, C. (2010). "Numerical simulation of wood diaphragm in concrete and timber hybrid structure," *Journal of Tongji University (Natural Science Edition* 38(10), 1414-1420. DOI: 10.3969/j.issn.0253-374x.2010.10.003

Liu, Q., and Yang, J. (1997). "The pseudo-plate method for the design of large span rib floor," *Building Science* 6, 30-34.

Liu, Y., Wang, H., Ding, P., and Song, Y. (2017). "The physical and mechanical properties of the poplar LVL," *China Forest Products Industry* 44(02), 12-16. DOI: 10.19531/j.issn1001-5299201702003

Liu, Y, Chen, J., Ma, H., Gong, M., and Zhang, L. (2022). "Mechanical performance of three types of connections used in orthogonal ribbed beams made of poplar LVL," *BioResources* 17(3), 4638-4655. DOI:10.15376/biores.17.3.4638-4655

Ma, H., Wang, J., Liu, M., Wan, Z., and Wang, K. (2019). "Experimental study of the behavior of beam-column connections with expanded beam flanges," *Steel and Composite Structures* 31(3), 319-327. DOI:10.12989/scs.2019.31.3.319

Ma, H., Zheng, H., Zhang, W., and Tang, Z. (2020). "Experimental and numerical study of mechanical properties for the double-ribbed reinforced beam-column connection," *Advanced Steel Construction*, 16(4), 297-309.DOI:10.18057/IJASC.2020.16.4.2.

Meng, F., Wu, B., She, Y., and Yu, W. (2016). "Effect of thicker veneers on properties of laminated veneer lumber," *China Wood Industry* 30(03), 5-8. DOI: 10.19455/j.mcgy.2016.03.001

Paquette, J., and Bruneau, M. (2006). "Pseudo-dynamic testing of unreinforced masonry building with flexible diaphragm and comparison with existing procedures," *Construction and Building Materials* 20(4), 220-228. DOI: 10.1016/j.conbuildmat.2005.08.025

Pathak, R., and Charney, F. A. (2008). "The effects of diaphragm flexibility on the seismic performance of light frame wood structures," in: *The 14th World Conference on Earthquake Engineering*, 12-17 October, Beijing, China, pp. 1-8.

Sadashiva, V. K., Macrae, G. A., and Deam, B. L. (2011). "A mechanics based approach to quantify diaphragm flexibility effects," in: *Proceedings of the Ninth Pacific Conference on Earthquake Engineering, Building an Earthquake-Resilient Society*, Auckland.

Shen, P. (2003). *Design Principle of Floor Structure*, Science Press, Beijing, China.

bioresources.com

Wang, Q., Shi, Q., Lui, M., and Xu, Z. (2019). "Axial compressive behavior of reactive powder concrete-filled circular steel tube stub columns," *Journal of Constructional Steel Research* 153, 42-54. DOI: 10.1016/j.jcsr.2018.09.032

Zhou, H., Jiang, Z., Fei, B., Ren, H., and Hu, L.(2008). "Study on vibration performance of engineered wood truss joist floors," *Journal of Chongqing Jianzhu University* 30(4), 109-113.